THE INFLUENCE OF LOW DENSITY BEHAVIOUR OF STATE EQUATION ON LATTICE INVERTED PAIR POTENTIAL FOR LEAD

ROBERT LASKOWSKI AND MIECZYSŁAW CHYBICKI

Department of Solid State Physics,
Faculty of Technical Physics and Applied Mathematics,
Technical University of Gdansk,
Narutowicza 11/12, 80–952 Gdansk, Poland

Abstract: A pair potential for lead (Pb) is extracted from the ab–initio energy–volume data using the lattice inversion procedure of Carlsson and co–workers [*Phil. Mag.* **41** (1980), p. 241]. Because of a limited accuracy of the ab–initio techniques, we extrapolate the energy–volume data for low–density systems with suitable analytical tail functions. We discuss the dependence of the molecular dynamics (MD) simulation structural results and the elastic modules on the choice of the cohesive energy tail function. The MD–simulated radial distribution functions (RDFs), obtained for several energy tails, in several temperatures are discussed.

Keywords: lattice inversion technique, pair potential, molecular simulations

1. Introduction

Although it is well known that the range of applicability of pairs potentials in the study of crystal properties is rather limited, the pair potentials are still the simplest and widely used way of describing the interaction energy between atoms as a function of their separation. Many functional forms of pair potentials are known. Most of them require an adjustment of some parameters, which can be determined by fitting various calculated thermodinamical or mechanical quantities to their experimental values. One the most appealing is the idea of the parameters–free ab–initio pair potential, first suggested by Carlsson, Gelatt, and Ehnreich [1]. Here the pair potential is constructed only on the basis of the energy–volume data obtained by the first principles calculation. In the case of analytical state equations, a method using the Mobius transformation [2–4] is most useful. The method, called the lattice inversion method, has gained same applications to metallic systems with pair potential interactions [5–7], and embedded atom type interactions [8–10].

The procedure of the pair potential construction requires the calculation of cohesion energy as a function of the structure deformation. Commonly available ab–initio techniques, due to numerous approximations to the exact quantum

mechanical formulation, do not allow to determine exactly the cohesive energy, especially in the case of heavy metals and/or strong lattice deformations. The most popular and possibly the only practical way of the energy calculation is the density functional theory (DFT). The exact formulation of DFT was made by Hohenberg, Kohn and Sham [11, 12], who have proposed the local density approximation (LDA) for the many–body exchange–correlation interactions. The DFT has been also extended to open–shell systems and magnetic solids [13, 14]. In this case, the exchange–correlation energy depends on the local spin density (the local spin density approximation — LSDA). The extension of LDA and LSDA, and the improvement of the calculation accuracy, can be accomplished by inclusion of non–local gradient corrections for the exchange–correlation energy [15, 16]. The energy calculations within the lowest level of approximation (DFT with non–local exchange–correlation potentials) can give results within about 0.1 eV off the experimental values. In our case, however, where the cohesive energy must be determined for many lattice deformations, such methods are computationally inefficient. Some approximations in the calculation can considerably lower the computational time. Although this may decrease the accuracy, the curvature of the energy–volume dependence near the equilibrium is often given rather well.

Because the extraction procedure demands the energy data for volumes much larger than are available within the ab–initio methods, the energy–volume dependence must be extrapolated by a suitable tail function (e.g. [1]). However, according to the authors knowledge, no systematic investigations of an influence of the particular shape of the tail function on the detailed form of pair potential and what follows spatial atom correlations have been undertaken. Such a discussion, focused on solid and liquid lead (Pb), is the subject of the present work.

The paper is organised as follows. In Section 2, we describe our approach to the pair potential construction. In Sections 3, we give the brief descriptions of our ab–initio calculations. In Section 4, the effective pair potential for Pb is constructed for several tail functions and the influence of the tail on molecular dynamics (MD) calculated radial distribution function (RDF) and elastic modules is presented. Section 5 contains concluding remarks.

2. The method of pair potential construction

Formally, in the case of a pair potential the cohesive energy per atom in a monatomic structure is represented by the sum over all the pairs of atoms:

$$E_{coh}(p) = \frac{1}{2} \sum_{R_p \neq 0} \Phi(|R_p|), \tag{1}$$

where R_p are the lattice vectors, p stands for parameters describing a deformation of the structure (symmetry of the unit cell is maintained, but its volume changes). Although the existence of Φ cannot be proven for an arbitrary structure and function $E_{coh}(p)$, the effective algorithms [1, 2] for the extraction of $\Phi(R)$ from $E_{coh}(p)$ are known for isotropic deformations.

In principle, having the energy–volume data for a crystal, one can construct the effective pair interaction potential. The potential extraction procedure consists in a simple inversion of relation (1). If one rewrites the interatomic separation R_p appearing in equation (1) as $S_i r$, where i stands for neighbouring shell index and r is the nearest neighbour distance, equation (1) obtains the following form:

$$E_{coh}(r) = \frac{1}{2}\sum_i W_i \Phi(S_i r), \tag{2}$$

where W_i is the number of atoms in the i–th neighbouring shell, and r depends on the atomic volume (exactly speaking r defines here the deformation of the FCC lattice). The right side of expression (2) defines an operator Θ such that:

$$E_{coh} = \Theta\Phi(r). \tag{3}$$

If one defines an operator Θ_i such that:

$$\Theta_i f(r) = \frac{1}{2} W_i f(S_i r),$$

the operator is just the sum of Θ_i over neighbouring shell indices i:

$$E_{coh} = \sum_i \Theta_i .$$

The expression for the pair potential $\phi(r)$ can be written as the inversion of equation (3):

$$\Phi(r) = \Theta^{-1} E_{coh}(r),$$

where Θ^{-1} denotes the inversion of operator Θ. Because Θ is the sum of Θ_i's, its inversion can be written as:

$$\Theta^{-1} = (I + \Theta_1^{-1}\sum_{i\neq 1}\Theta_i)^{-1}\Theta_1^{-1}, \tag{4}$$

where Θ_i^{-1} is the inversion of Θ_i:

$$\Theta_i^{-1} f(r) = \frac{2}{W_i} f\left(\frac{r}{S_i}\right).$$

The second term in parenthesis in equation (4) is treated as a perturbation, and the whole expression can be expanded in a Taylor series. In our calculations we sum the Taylor series up to 20 elements, which ensures a very good convergence of the series. The resulting pair potential substituted to equation (1) reproduces exactly the ab–initio energy–volume curve.

Because the extraction procedure demands energy data for the volumes much larger than used in our calculations (see next section), we extrapolate it by a tail function defined as:

$$T(r) = A_1 e^{(A_2 r + A_3 r^2 + A_4 r^{**})}. \tag{5}$$

The parameters A_1, A_2, A_3 are chosen to ensure the continuity conditions between the cohesive energy data and the tail function for their values, and their first and second derivatives. We extrapolate the ab–initio data also for the low volumes (in a similar way), but this affects the pair potentials only at much lower distances than the nearest neighbour equilibrium distance, and therefore has only minor influence on the MD simulation results. A_4 and w are allowed to change freely despite of the constraint $w > 2$. In Sections 4 the pair potential is constructed for $w = 3$ and A_4 changing from 0 to –20.

3. State equation calculation details

Our ab–initio calculations of state equation for Pb were performed in the density functional theory [11, 12] (DFT) framework. We used ESOCS 4.0 program [17]. ESOCS uses the parameterized form of the local spin density (LSD) approximation of the exchange–correlation energy given by Hedin and Lundquist [18] and von Barth and Hedin [13]. The scalar relativistic approximation of Koelling and Harmon [19] and the spin orbit coupling Andersen [20] is used to include the relativistic effects. The form of the spin orbit hamiltonian was proposed by MacDonald et al. [21]. The atomic sphere approximation (ASA) introduced by Andersen [20] with necessary correction terms is also included into the approximation scheme. The basis set used by ESOCS is a type of linear combination of atomic orbitals (LCAO) with minimal set of accurate "muffin–tin" type orbitals [20]. The standard Monkhorst and Pack [22] method is used to generate the k–point integration mesh. In our calculation, the real space cut–off distance of the k–point set was equal to 50 Å. The approximations used here are

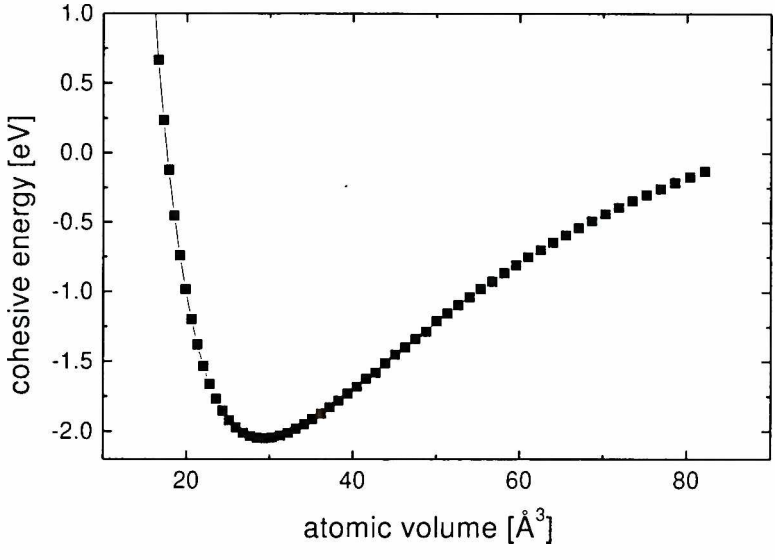

Figure 1. *The ab-initio calculated total energy vs volume for Pb in FCC phase. The curves are shifted in energy scale to give experimental value of cohesive energy (2.05 eV)*

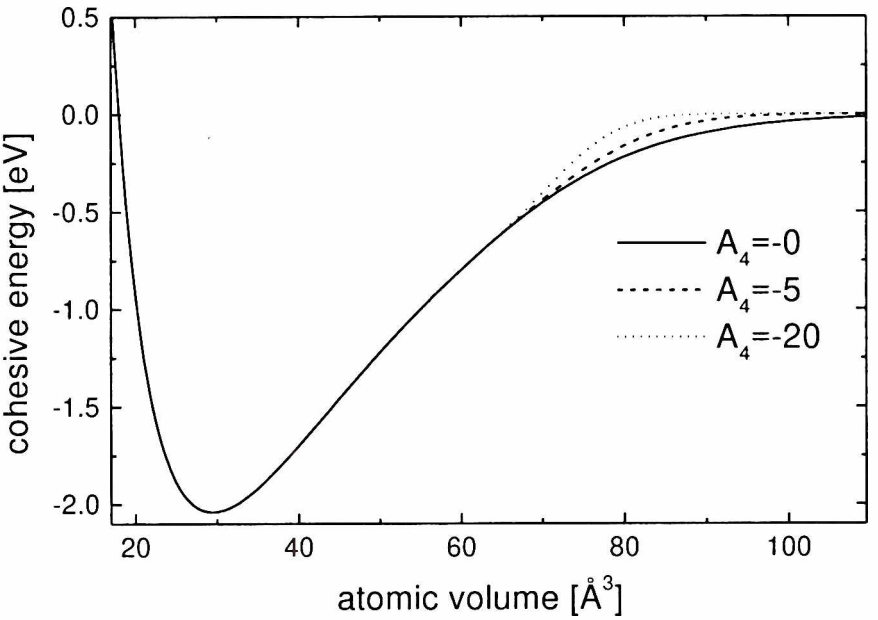

Figure 2. The ab-initio energy vs atomic volume augmented by the tails calculated for w = 3 (see equation (5))

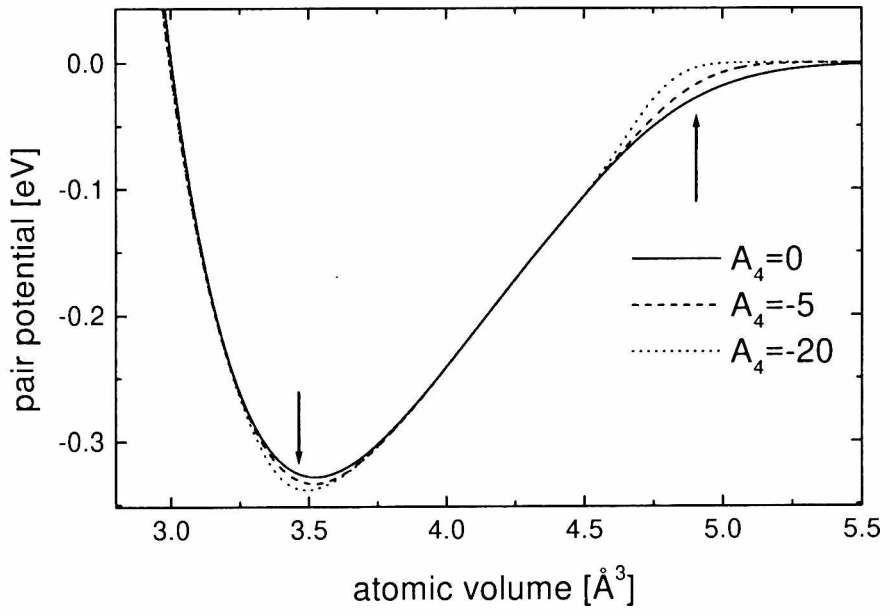

Figure 3. *Pair potentials extracted from the cohesive energy curves plotted in Figure 2 (arrows point to the distances of first and second coordinating shells)*

considered to give good results in their application to the close packed materials with minimal computational efforts.

The calculations of total energy were done for the face–centred cubic (FCC) lattice in the range of atomic volumes 10–80 Å^3. Figure 1 contains the results. Since we have calculated the total energy, the curve has been shifted in the energy scale to match the experimental value of the cohesive energy (2.05 eV). As one can note, the equilibrium zero temperature atomic volume for our calculations is about 29.3 Å^3. This gives the lattice constant equal to 4.90 Å. The experimental value of lattice constant, extrapolated to zero temperature, is about 4.84 Å [23]. The bulk modulus, evaluated by differentiating of the energy versus volume relation at the equilibrium volume equals to 0.532 Mbar, whereas the experimental value extrapolated to 0 K [23] equals to 0.488 Mbar.

4. Results

In order to test an influence of the tail functions on the pair potential shape and the resulting properties of metal, we extrapolate our ab–initio data by tails with w (see equation (5)) equal to 3 and A_4 equal to 0, –2, –5, –10, and –20. We have also tested tail functions with $w = 4$ and $w = 5$, but the results have appeared to be qualitatively the same as for $w = 3$, and they do not change the final conclusions. Figure 2 presents cohesive energy vs volume curves, extrapolated by our tails. The resulting potentials are plotted in Figure 3. It is seen, that the decrease of A_4 results in deeper, and faster going to zero potentials. Small shift of the potential minimum towards lower distances is also seen.

Potential approximation allows us to calculate almost all properties of solid Pb. Here we concentrate ourselves on elastic modules and MD–calculated radial distribution functions. Table I presents the calculated and experimental values of bulk module (B), C_{11}, C_{12} and C_{44}. We can see that the calculated values of C_{11}, C_{12}

Table I. *Zero temperature experimental [23] and potential-calculated values of the elastic modules*

	C_{11}	C_{12}	C_{44}	B
experiment	0.555	0.454	0.194	0.488
$A_4 = 0$	0.543	0.523	0.526	0.532
$A_4 = -2$	0.485	0.555	0.555	0.532
$A_4 = -5$	0.380	0.608	0.608	0.532
$A_4 = -10$	0.234	0.680	0.680	0.532
$A_4 = -20$	0.173	0.710	0.710	0.532

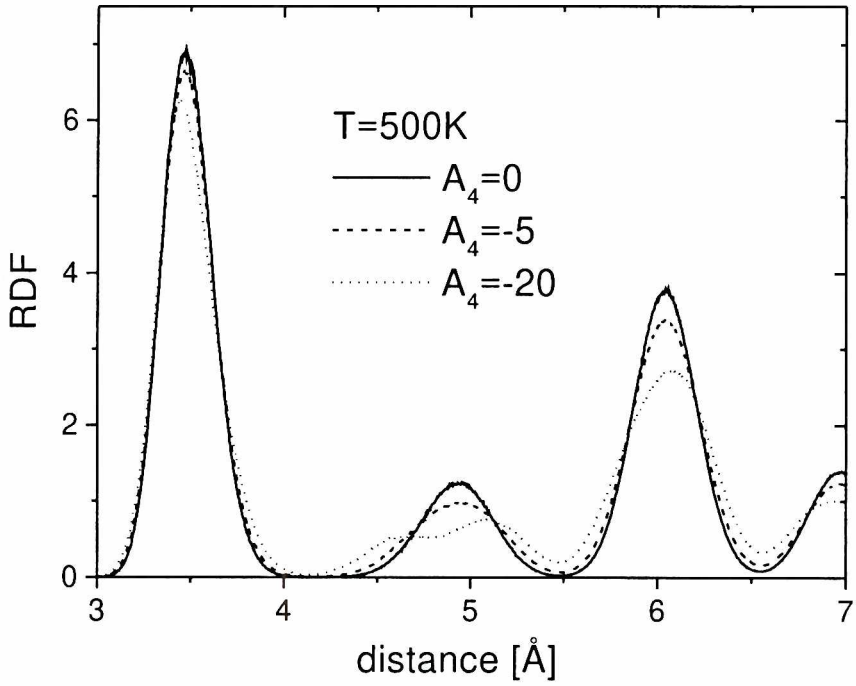

Figure 4. *MD calculated RDFs for the potentials of Figure 3. Temperature equal to 500 K*

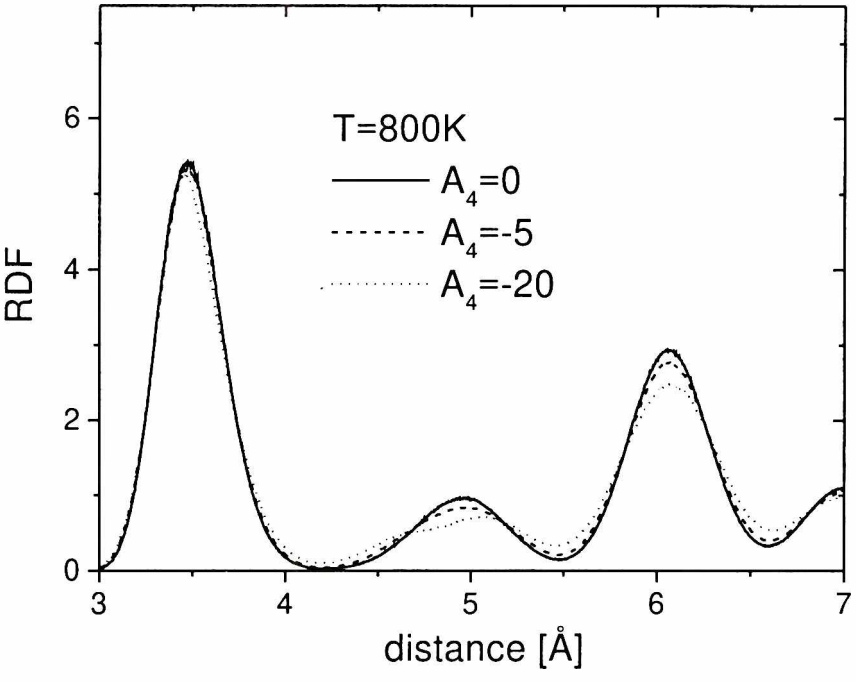

Figure 5. *MD calculated RDFs for the potentials of Figure 3. Temperature equal to 800 K*

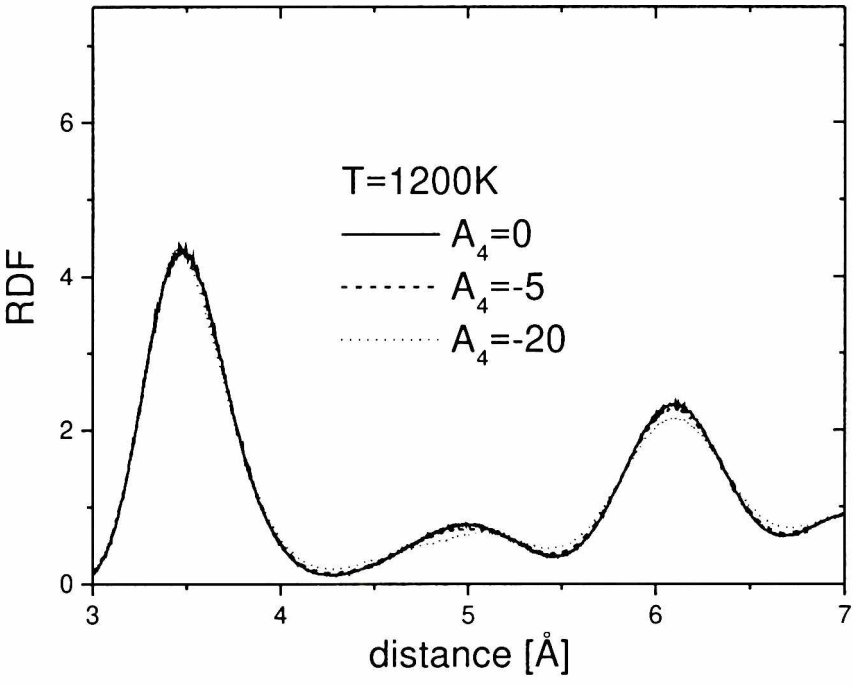

Figure 6. *MD calculated RDFs for the potentials of Figure 3. Temperature equal to 1200 K*

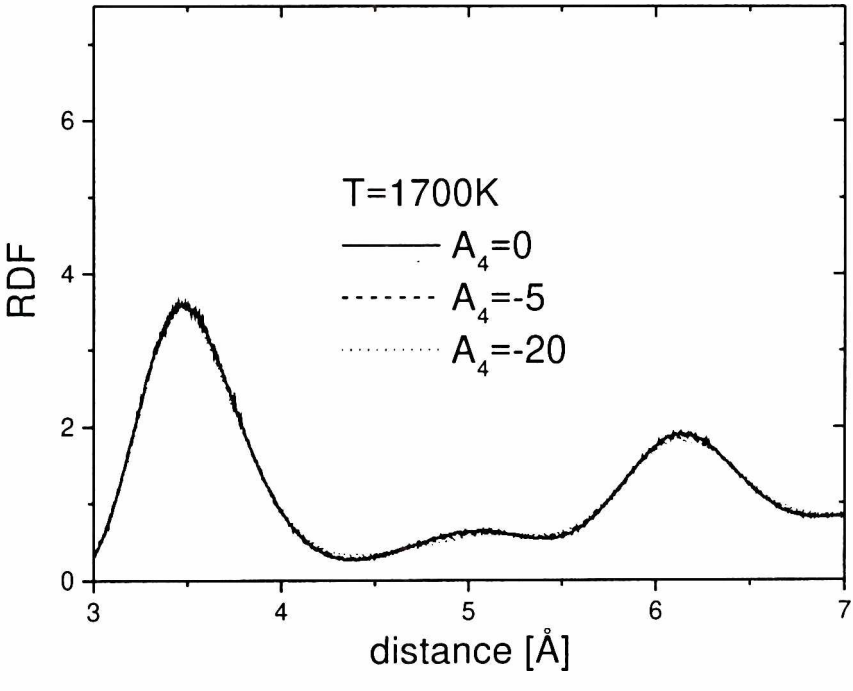

Figure 7. *MD calculated RDFs for the potentials of Figure 3. Temperature equal to 1700 K*

and C_{44} are considerably sensitive to the tail shapes. With decreasing A_4, the values of C_{11} decrease, while those of C_{12} and C_{44} increase. One should notice that for all potentials C_{12} is equal to C_{44}, what is well known defect of pair potential approximation. Because the curvature of the state equation at equilibrium volume does not depend on the tails, the bulk modulus B is equal for all potentials.

All the RDFs have been calculated in the NPT ensemble at the temperatures of 500 K, 800 K, 1200 K, 1700 K. The simulation cell contained 864 particles, which was sufficient regarding the cut–off distance of our potentials (only 6 Å, see Figure 3). Equation of motion has been integrated using standard leap–frog algorithm with time step equal to 2 fs. We have equilibrated the samples by 10000 time steps. During the next 10000 steps, RDFs have been accumulated.

The MD–calculated RDFs are presented in Figures 4–7. The dependence of the RDFs calculated at lower temperatures on the shape of the potentials is evident (see Figures 4 and 5). For the potentials slowly approaching zero all the RDF peaks are higher and narrower. The decrease of parameter A_4 (deep and short–range potentials) lowers and broadens the RDFs. This tendency is probably the result of the shift of the potential minimum and the change of its slope at the nearest neighbour distance. For a given thermal energy, greater vibrational amplitudes are expected for lower A_4 values. An analysis of a volume accessible to any atom that moves in the cage constructed by its nearest neighbours confirms this conclusion. The rate of the change of each peak of RDF is different. The first peak seems to be least sensitive. The height of the third peak changes most significantly (from about 3.7 for $A_4 = 0$ to 2.7 for $A_4 = -20$). At the same time the second peak besides its height changes also its shape. For $A_4 = -20$, as we see from Figures 4 and 5, this peak splits into two sub–peaks. Closer analysis of the structure shows that system simply changes its phase. If simulation is performed in constant stress ensemble, the BCC phase replaces the FCC phase. In the case of constant volume or constant pressure ensembles, only a part of the atoms has BCC–like neighbourhoods, which can be detected using the Voronoi polyhedra contraction technique [24, 25]. The dependence of the RDFs on the tail shapes is not so strong in higher temperatures (it vanishes completely in very high temperatures). We can see that for the temperature of 1200 K (Figure 6) it is rather small, whereas for the temperature 1700 K the RDFs calculated for all potentials are practically identical.

6. Concluding remarks

The ab–initio calculations can not provide the exact energy–volume dependence for the volume range, needed to the pair potential extraction procedure. Thus, a suitable extrapolation of the ab–initio data is necessary. As it is seen above, the MD calculated RDFs and elastic modules (except bulk modulus) strongly depend on the type of the energy tail function. Considering the calculated C_{11} and C_{12} we see that potentials constructed from the state equation extrapolated by tails with the highest A_4 gives the values of elastic modules closest to the experiment. These potentials give also stable FCC phase. Decreasing A_4 cause in considerable

decreasing of C_{11}, increasing of C_{12} and C_{44}, and also destabilisation of FCC phase (the splitting of the RDF second peak). Because of the sensitivity of the peak height and the elastic modules on A_4 (and also on w), it is possible to optimise the tail function in such a way that the constructed pair potentials lead to the matching between the experimental and the calculated properties. For solid rhodium (Rh), we have performed this type of optimisation [26]. In the case of the first RDF peak, this matching is almost exact. However, the heights of the second, third, and fourth MD–simulated RDF peaks are at the lower limit of the band defined by the error bar on the experimental data (EXAFS).

Acknowledgements

The opportunity to perform our numerical calculations at the TASK Computer Centre (Gdansk, Poland) is kindly acknowledged. Support for this work was provided by KBN, Poland under grant No. 2P03B03016.

References

[1] A. E. Carlsson, C. D. Gelatt and H. Ehrenreich, *Phil. Mag.* **41** 241 (1980)
[2] N. X. Chen, *Phys. Rev. Lett.* **64** 1193 (1990)
[3] N. X. Chen and G. B. Ren, *Phys. Rev.* **B 45** 8177 (1992)
[4] N. X. Chen, Z. Chen, Y. Shen, S. Liu and M. Li, *Phys. Lett.* **A 184** 347 (1994)
[5] A. Mookerjee, N. Chen, V. Kumar and M. A. Satter, *J. Phys.* CM **4** 2439 (1992)
[6] M. Li, S. J. Liu, N. X. Chen, Y. Teng, W. X. Zheng and S. Z. Zhong, *Phys.Lett.* **A 169** 394 (1992)
[7] W. Q. Zhang, Q. Xie, J. G. Xi and N. X. Chen, *J. Appl. Phys.* **82** 578 (1997)
[8] Q. Xie and M. Huang, *J. Phys.* CM **6** 11015 (1994)
[9] Q. Xie and M. Huang M, *Physica status solidi* (b) **186** 393 (1994)
[10] Q. Xie and N. Chen, *Phys. Rev.* **B 51** 15856 (1995)
[11] P. Hohenberg and W. Kohn, *Phys. Rev.* **136** B864 (1964)
[12] W. Kohn and L. J. Sham L J, *Phys. Rev.* **140** A1133 (1965)
[13] U. von Barth and L. J. Hedin L J, *Physica* **C 5** 1629 (1972)
[14] O. Gunnarsoson, B. I. Lundqvist and S. Lundqvist, *Solid State Commun.* **11** 149 (1972)
[15] J. P. Pedrew, *Phys. Rev.* **B 33** 8822 (1986)
[16] A. D. Becke, *Phys. Rev.* **A 38** 3098 (1988)
[17] ESOCS is a part of Castep package provided by MSI (*www.msi.com*)
[18] L. Hedin, B. I. Lundquist, *J. Phys.* **C 4**, 2064 (1971)
[19] D. D. Koelling, B. N. Harmon, *J. Phys.* **C 10**, 3107 (1977)
[20] O. K. Andersen, *Phys. Rev.* **B 12**, 3060 (1975)
[21] A. H. MacDonald, W. F. Pickett, D. D. Koelling, *J. Phys.* **C 13**, 2675 (1980)
[22] H. J. Monkhorst, J. D. Pack, *Phys. Rev.* **B 13**, 5188 (1976)
[23] C. Kittel, *Introduction to Solid State Physics* (PWN, Warszawa 1999)
[24] R. Laskowski, J. Rybicki and M. Chybicki, *TASK Quart.* **1** 96 (1997)
[25] W. Brostow, M. Chybicki, R. Laskowski and J. Rybicki, *Phys. Rev.* **B 57** 13448 (1998)
[26] R. Laskowski, J. Rybicki, M. Chybicki and A. Di Cicco, *Physica status solidi* (b) (1999) (in print)